Thermal Stability and Decomposition Products of Hexabromocyclododecane

ARTICLE *in* INDUSTRIAL & ENGINEERING CHEMISTRY RESEARCH · JUNE 2001

Impact Factor: 2.59 · DOI: 10.1021/ie001002v

3 AUTHORS, INCLUDING:

Federica Barontini
Università di Pisa
55 PUBLICATIONS **920** CITATIONS
SEE PROFILE

Luigi Petarca
Università di Pisa
45 PUBLICATIONS **1,071** CITATIONS
SEE PROFILE

Thermal Stability and Decomposition Products of Hexabromocyclododecane

Federica Barontini,[†] Valerio Cozzani,[*,‡] and Luigi Petarca[‡]

Gruppo Nazionale per la Difesa dai Rischi Chimico-Industriali ed Ecologici, Consiglio Nazionale delle Ricerche, via Diotisalvi n.2, 56126 Pisa, Italy, and Dipartimento di Ingegneria Chimica, Chimica Industriale e Scienza dei Materiali, Università degli Studi di Pisa, via Diotisalvi n.2, 56126 Pisa, Italy

The thermal stability and decomposition products of hexabromocyclododecane (HBCD), a widely used aliphatic brominated flame retardant, were investigated. HBCD thermal degradation was carried out in nitrogen and in air at moderate heating rates (10 °C/min) using thermogravimetric analyzers and a laboratory-scale fixed-bed reactor. The identification of decomposition products was based mainly on FTIR and gas-chromatographic/mass-spectrometric techniques. Quantitative data on hydrogen bromide formation and on the bromine distribution among the different product fractions were obtained. For the experimental conditions used in this study, about 75 wt % of the bromine is released as HBr, and 25 wt % is involved in the formation of high-molecular-weight bromo-organic compounds. The main pathways of HBCD thermal degradation were assessed, and a global mechanism for HBCD decomposition was proposed.

Introduction

Additive and reactive brominated flame retardants are widely used in industrial practice to improve the resistance of polymeric materials.[1] In particular, products containing more than 20% bromine by weight are commonly used for the production of computer electronic boards. However, concern is growing about the possible formation of hazardous products in the thermal degradation of these substances. In particular, fires involving polymeric materials containing brominated fire retardants and runaway accidents during the production of these materials are suspected of potentially leading to the formation of brominated polyaromatic compounds, such as polybrominated dioxins.

In recent years, at least four accidents have been reported involving batch reactors during the production of brominated epoxy resins. The presence of brominated flame retardants caused the release of clouds of toxic products, possibly including hydrogen bromide, bromophenols, and other hazardous brominated compounds.

However, even though a vast literature is available on the mechanisms of formation of chlorinated polyaromatic structures, less attention has been devoted to the brominated homologues. The studies performed in the past 15 years have mainly concerned the formation of polybrominated dibenzofurans (PBDFs) and dibenzodioxins (PBDDs) in the thermal degradation of polybrominated diphenyl ether flame retardants.[2−12]

Limited data are available on the decomposition products of aliphatic brominated flame retardants. Hexabromocyclododecane (HBCD) is the most important of these products from an industrial point of view.[1] Several studies[13−16] have concentrated mainly on the thermal stability of this compound. The thermal degradation and combustion products of HBCD in polymer matrixes were investigated by Dumler et al.[5] However, no systematic analysis was undertaken concerning the distribution of bromine among the different product fractions of HBCD thermal degradation or combustion. Furthermore, limited data are available on the formation pathways of high-molecular-weight decomposition products of HBCD in inert or oxidizing atmospheres.

Table 1. Bromine Content, Melting Point Estimated from DSC Data, and Isomeric Composition of HBCD Samples

	bromine content (%)	melting point (°C)	isomeric composition		
			α isomer (%)	β isomer (%)	γ isomer (%)
HBCD1	74.59	189.0	2.0	10.1	87.9
HBCD2	71.87	182.7	nd[a]	nd[a]	nd[a]
HBCD3	74.65	205.7	0	0	100

[a] Not determined.

This study focused on the characterization of HBCD thermal degradation in both inert and oxidizing environments. HBCD decomposition was carried out at moderate heating rates (10 °C/min) using thermogravimetric analyzers and a laboratory-scale fixed-bed reactor. The identification of decomposition products was based mainly on FTIR and gas-chromatographic/mass-spectrometric (GC/MS) techniques.

The experimental work was aimed at investigating the distribution of bromine among the gaseous and condensable decomposition products. The data obtained shed some light on the pathways of HBCD decomposition and on the mechanisms for the possible formation of polyaromatic brominated compounds.

Experimental Section

Materials. 1,2,5,6,9,10-Hexabromocyclododecane (HBCD) samples from two different suppliers were used in the present work. HBCD1 was provided by Aldrich (Milan) and HBCD2 by Fluka (Milan). Table 1 reports the bromine contents determined by the suppliers. The table also reports the melting points of the two samples,

* Author to whom correspondence should be addressed. Tel.: (+39)-050-511212. Fax: (+39)-050-511266. E-mail: v.cozzani@ing.unipi.it.

[†] Consiglio Nazionale delle Ricerche.

[‡] Università degli Studi di Pisa.

10.1021/ie001002v CCC: $20.00
Published on Web 06/23/2001

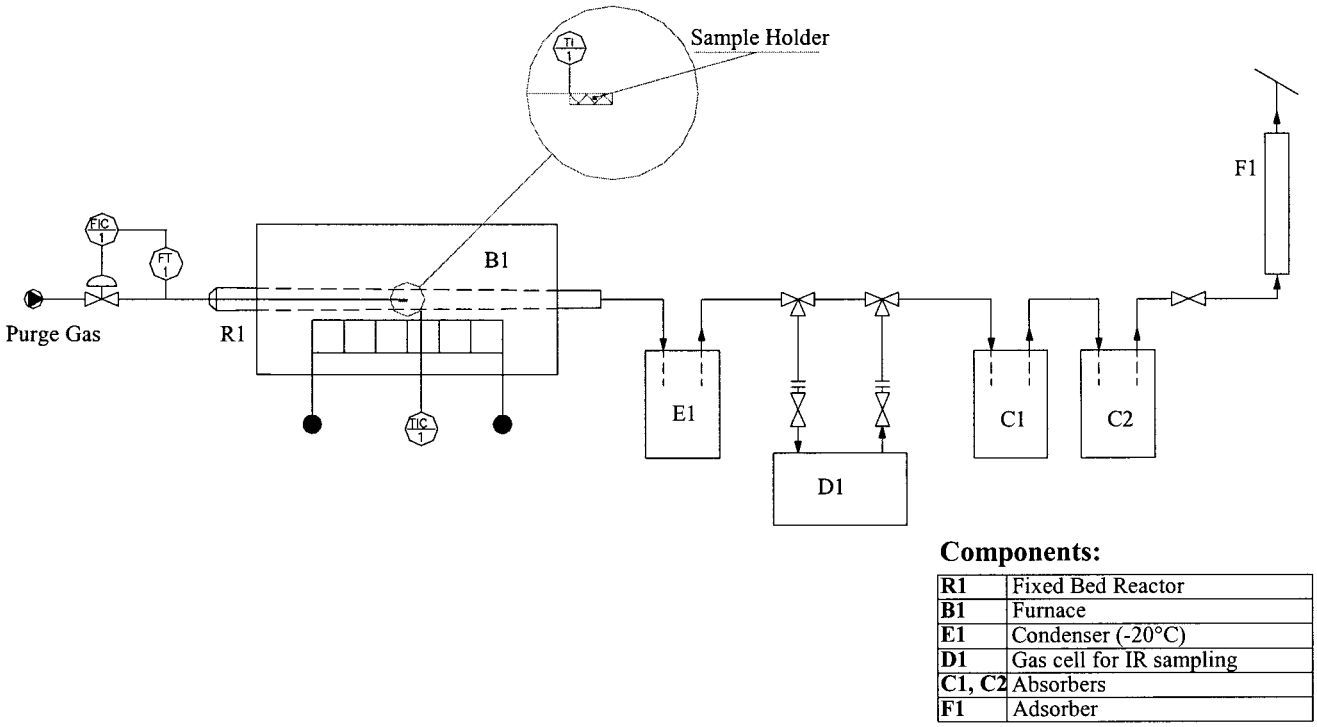

Figure 1. Scheme of the fixed-bed reactor (FBR).

as estimated by experimental differential scanning calorimetry (DSC) measurements.

To obtain a HBCD sample of higher purity, the leaching procedure suggested by Larsen[13] was applied. According to this procedure, 500 mg of HBCD1 was completely dissolved in 30 mL of dichloromethane. Then, 30 mL of methanol was added, and crystallization occurred. After 12 h, the crystals were filtered and dried, yielding 260 mg of solid. The same process was repeated with 160 mg of the crystals, resulting in about 100 mg of dry solid, denoted HBCD3 in the following.

Techniques. A Mettler DSC-25 calorimeter was used for melting point determinations. A constant heating rate of 10 °C/min, typical sample weights of 5−6 mg, and a pure nitrogen purge flow of 300 mL/min were used in the experimental runs. The melting point was approximated as the onset temperature of the corresponding endothermic peak, evaluated from experimental DSC runs.

Simultaneous thermogravimetric (TG) and DSC data were obtained using a Netzsch STA 409/C thermoanalyzer. A constant heating rate of 10 °C/min (0.167 °C/s) was used in the experimental runs. Typical sample weights of 5−15 mg and alumina crucibles were employed. The atmosphere surrounding the samples was controlled using a continuous purge gas flow (60 mL/min). Experimental runs were carried out using pure nitrogen or air (21 mol % oxygen).

Isothermal runs at temperatures between 200 and 300 °C were performed using a Mettler TG-25 thermobalance. Alumina crucibles and typical sample weights of 3−5 mg were used in the experimental runs. The samples were positioned on the pan of the TG balance and were inserted in the TG furnace that was preheated at the programmed temperature. A pure nitrogen purge flow rate of 200 mL/min was used in the experimental runs to prevent sample oxidation and to remove gaseous pyrolysis products. Temperature transients due to sample heating were calculated accounting for convective and conductive heat transfer inside the cylindrical furnace[17] and resulted in less than 30 s at temperatures between 200 and 400 °C.

FTIR measurements were carried out using a Bruker Equinox 55 spectrometer equipped with DTGS and MCT detectors.

TG-FTIR simultaneous measurements for the on-line analysis of volatile compounds formed during the TG runs were carried out by coupling the FTIR spectrometer to the Netzsch TG instrument using a 2-mm-internal-diameter Teflon tube. The 800-mm-long transfer line and the head of the TG balance were heated at a constant temperature of 200 °C to limit the condensation of volatile decomposition products. FTIR measurements were carried out with a MCT detector in a specifically developed low-volume gas cell (8.7 mL) with a 123-mm path length, heated at a constant temperature of 250 °C. The gas flow from the TG outlet to the IR gas cell was 60 mL/min, and a residence time of 30 s in the transfer line could be evaluated for the evolved gases. This value was assumed to be the time delay correction used for the comparison of TG and IR results. During TG-FTIR runs, spectra were collected at 4 cm^{-1} resolution, with the co-addition of 16 scans per spectrum. This resulted in a temporal resolution of 9.5 s, more than sufficient to follow the gas evolution rates characteristic of TG runs at heating rates of 10 °C/min.

A laboratory-scale fixed-bed reactor (FBR) was used to carry out HBCD thermal decomposition runs in inert and oxidizing atmospheres. The experiments were mainly aimed at the recovery and characterization of the gaseous and condensable fractions of the volatile decomposition products. The scheme of the FBR is shown in Figure 1. The sample was positioned on the sample holder and inserted in the temperature-controlled furnace at the beginning of the run. Experimental runs were performed using a continuous purge gas flow to control the reaction environment and to limit the extent of secondary gas-phase reactions. A conden-

sate trap (E1 in the figure), maintained at −20 °C by a sodium chloride brine, allowed for the recovery of condensate samples. The condensate trap was followed by a gas sampling cell (D1 in the figure; volume = 160 mL, optical path length = 100 mm) for off-line gas analysis by FTIR spectroscopy. The gas then flowed into two absorbers (C1 and C2 in Figure 1) containing a sodium hydroxide standard solution to allow the absorption of gas-phase acidic compounds.

A Fisons MD 800 mass spectrometer interfaced to a Fisons GC-8060 gas chromatograph was used for GC/MS analysis. The GC was equipped with a Mega SE30 fused-silica capillary column (25-m length, 0.32-mm i.d., cross-linked, 0.25-μm film thickness). The column temperature program was the following: 5 min isothermal at 40 °C, heating to 250 °C (2.5 °C/min), and then 20 min isothermal. Helium was used as the carrier gas at a 2 mL/min constant flow rate. Splitless injection with the injector at 250 °C was used. Mass spectrometric detection was performed under full scan conditions (scan range, m/z 10−819) in electron-impact ionization mode.

High-performance liquid chromatography (HPLC) analysis was carried out on a Jasco PU-1580 chromatographic system, equipped with a Jasco UV-1575 detector (λ = 215 nm) and a Perkin-Elmer C18 column (3-cm length, 3-μm particle size) using acetonitrile/water 75/25 as the eluent at a 1 mL/min constant flow rate.

Procedures Used in FBR Experimental Runs. At the beginning of the run, 200−300 mg of sample were positioned in the sample holder. Sample heating rates of 10 °C/min were used, and a residence time of 10 min at the final temperature (usually 500 °C) was accomplished.

Experimental runs were performed under pure nitrogen or air (21 mol % oxygen) atmospheres, using a 6 L/h purge gas flow rate. Samples of condensable products for GC/MS analysis were recovered at the end of the run from the condensate trap (E1 in Figure 1). During experimental runs, FTIR spectra of the gaseous products evolved were recorded at 5-min intervals in the D1 gas sampling cell (see Figure 1). At the end of each experimental run, absorbed acid compounds were quantitatively determined by titration of the C1 and C2 alkaline solution with a hydrochloric acid standard solution using phenolphthalein as the indicator. To detect the possible presence of molecular bromine, the collected solution was also checked by the fluorescein test[18] and by iodometric titration.[19]

Qualitative Gas Evolution Profiles from TG-FTIR Runs. A linear relation between the spectral absorbance at a given wavenumber and the concentration of a gaseous compound is postulated by the Lambert−Beer law. However, because of the limited resolution of FTIR measurements, the Lambert−Beer relation is generally used in an integral form over a characteristic wavenumber interval

$$I = \int_{\nu_1}^{\nu_2} A(\nu)\, \mathrm{d}\nu = \int_{\nu_1}^{\nu_2} \epsilon(\nu) l C\, \mathrm{d}\nu = KC \qquad (1)$$

where I is the integral value, A is the measured absorbance, ϵ is the extinction coefficient of the gaseous compound, l is the optical path length used in the measurement, C is the concentration, and (ν_1, ν_2) is the wavenumber interval selected for the measurement. K is a constant that should be independent of concentration if deviations from the Lambert−Beer law can be neglected, as discussed below. The value of K depends on the compound considered, the wavenumber interval, the temperature of the gas, the optical path length, and the instrument resolution. Thus, a reliable value of K can be obtained only by a calibration procedure. Nevertheless, even in the absence of experimental calibration, eq 1 shows that TG-FTIR measurements can be used to generate a specific gas profile to monitor qualitatively the evolution of a gas as a function of the time or of the temperature of the TG furnace. This requires that the compound of interest have a wavenumber absorption interval that is free of additional contributions from other substances. The contemporary formation of a wide number of volatile compounds complicates the selection of such intervals. The wavenumber intervals selected to obtain concentration profiles were the following: carbon monoxide, 2030−2235 cm^{-1}; carbon dioxide, 2240−2400 cm^{-1}; hydrogen bromide, 2498−2516 cm^{-1}; methane, 3001−3026 cm^{-1}; hydrocarbons, 2830−3150 cm^{-1}. Whereas for hydrogen bromide, carbon monoxide, and carbon dioxide, wavenumber intervals representative of the individual compounds were identified, for hydrocarbon compounds the wavenumber interval selected, corresponding to the C−H bond stretching region, should represent the global profile of all of the hydrocarbon species present in the measurement cell.

Quantitative Determination of Hydrogen Bromide in TG-FTIR Runs. The most important gaseous product formed in HBCD decomposition is hydrogen bromide (HBr). Thus, the results of the TG-FTIR runs were also analyzed to estimate the quantities of HBr formed during the thermal degradation in the TG analyzer.

The FTIR software allows for the integration of eq 1 with respect to time

$$D = \int_{t_1}^{t_2} \left[\int_{\nu_1}^{\nu_2} A(\nu)\, \mathrm{d}\nu \right] \mathrm{d}t = K \int_{t_1}^{t_2} C\, \mathrm{d}t \qquad (2)$$

where (t_1, t_2) is the interval in which the formation of the compound of interest takes place. The total amount, P, of the compound of interest evolved during the interval (t_1, t_2) can be expressed as

$$P = \int_{t_1}^{t_2} QC\, \mathrm{dt} \qquad (3)$$

where Q is the total volumetric gas flow rate at the actual gas temperature in the measurement cell.

If the total volumetric gas flow rate through the FTIR measurement cell is constant, the value of the integral in eq 2, D, is easily related to P via

$$P \approx Q \int_{t_1}^{t_2} C\, \mathrm{dt} = \frac{Q}{K} D \qquad (4)$$

Because a constant purge gas flow rate of 60 mL/min (at 25 °C) is used during the TG-FTIR runs, eq 4 is valid if the volumetric contribution of the volatiles generated during the TG run to the total volumetric flow rate can be neglected with respect to the purge gas flow, as is the case.

Thus, if the linear relation between the concentration and the absorbance given by eq 1 can be assumed over a selected wavenumber interval in the range of concentrations of interest, the FTIR absorption measurements can be used to estimate the amount of HBr formed during HBCD decomposition.

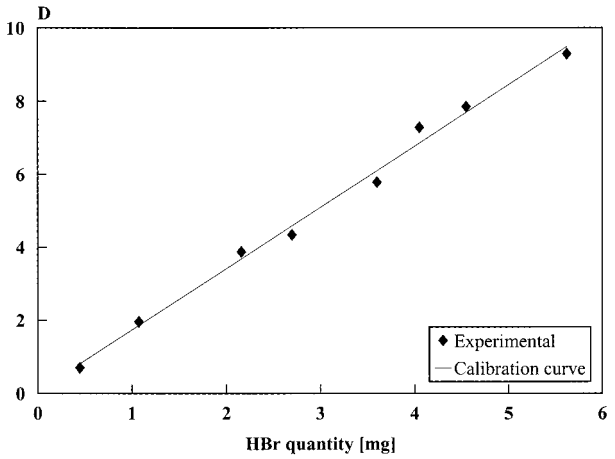

Figure 2. Calibration data used for the quantitative determination of HBr formed in HBCD decomposition during TG-FTIR runs.

Deviations from linearity might be caused mainly by the relatively low spectral resolution setting of the instrument (4 cm^{-1}) compared to the molecular spectral line width of the measured gases. The resolution chosen was a compromise between a spectral resolution allowing for the separation and identification of the different spectral features and a time resolution sufficiently high for the measurement of gas evolution profiles. Moreover, it was shown that nonlinear deviations can be neglected if a relatively narrow concentration range is considered, as is the case.[20,21]

To estimate the quantities of HBr evolved during HBCD decomposition, an experimental calibration was performed using HBr−water solutions with different HBr concentrations. Five HBr−water solutions were used, with the following HBr concentrations (% of HBr by weight): 2.8, 8.1, 15.4, 21.9, and 24.0. Different quantities (15−25 mg) of solution were vaporized in the TG apparatus during runs performed at a heating rate of 10 °C/min between 40 and 200 °C using a 60 mL/min pure nitrogen flow. The vaporization of HBr took place between 70 and 140 °C. This corresponds to a time interval of about 400 s using a constant heating rate of 10 °C/min. The value is quite close to the decomposition time of HBCD during constant-heating-rate runs at 10 °C/min, which was about 300 s, as shown in the following.

The value of the integral in eq 1, *I*, was calculated on the wavenumber interval selected for HBr (2498−2516 cm^{-1}) and was integrated with respect to time according to eq 2. The values obtained for the integral with respect to time, *D*, from the analysis of the experimental calibration runs are plotted in Figure 2 with respect to the amount of HBr present in the sample vaporized. As shown in the figure, a linear dependence of the value of *D* with respect to the HBr quantity was obtained from the experimental runs, thus suggesting that the error introduced by neglecting nonlinear phenomena can be accepted in the range of concentrations present during the experimental runs.

The best-fit linear relation between the value of *D* and the HBr quantity obtained from the calibration shown in Figure 2 was used to estimate the amount of HBr formed during HBCD thermal degradation in TG-FTIR runs. The reproducibility of the experimental quantitative hydrogen bromide measurements was tested using HBCD samples and water−HBr solutions.[22] Differences in the estimated values of the HBr quantities were less than 3 wt %.

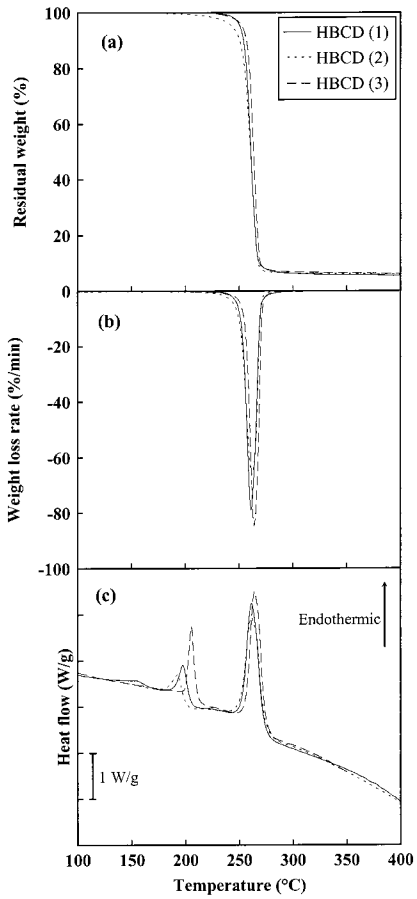

Figure 3. Results of simultaneous TG/DSC runs carried out on HBCD samples at a heating rate of 10 °C/min in 100% nitrogen: (a) TG data, (b) dTG data, (c) DSC data.

Results and Discussion

Characterization of HBCD Samples. Literature data suggest that the thermal stability of HBCD is influenced by impurities present in the material.[13,14,16] Some authors also suppose an influence of the isomeric composition of HBCD on the decomposition temperature,[13] although different opinions have been expressed on this point.[14,15] For these reasons, the HBCD samples were previously characterized to detect the presence of impurities and to obtain information on the quantities of the different HBCD isomers present.

GC/MS analyses were performed on the HBCD samples. Five isomers of tetrabromocyclododecene (TBCD), reported in the literature as a byproduct of HBCD synthesis, and of pentabromocyclododecene were detected. No other organic compound was present in the HBCD samples, at least within the sensitivity of the detection method used. HPLC runs were also performed, but the results did not provide evidence for the presence of impurities other than those previously mentioned. No significant differences resulted in the GC/MS chromatograms of samples HBCD1 and HBCD3, thus indicating that the purification procedure had a limited effectiveness for the separation of the organic impurities present in HBCD.

The results of DSC runs on HBCD1, HBCD2, and HBCD3 performed in 100% nitrogen at a heating rate of 10 °C/min are reported in Figure 3c. The estimated

melting points obtained from DSC data are reported in Table 1. It must be recalled that commercial HBCD is a mixture of three isomers (α, mp 172 °C; β, mp 169 °C; γ, mp 209 °C).[15] The results in Table 1 suggest that the purification procedure applied to obtain sample HBCD3 resulted in a higher content in the γ isomer. HPLC runs were performed on samples HBCD1 and HBCD3 to identify and quantify the different HBCD isomers. The results, reported in Table 1, confirmed this hypothesis. As shown in the table, sample HBCD3 was composed only of the γ isomer of HBCD.

Thermal Stability of HBCD. The results of constant-heating-rate runs performed on the three HBCD samples in the simultaneous TG/DSC analyzer are shown in Figure 3. The data reported in this and the following figures were calculated as the means of at least three experimental runs. Differences in weight loss or in heat flow with respect to temperature in different runs were less than 2%.

As widely reported in the literature, HBCD decomposition begins at temperatures around 230 °C. Figure 3a shows that the thermal degradation of HBCD takes place mainly between 240 and 270 °C if a heating rate of 10 °C/min is used. Limited differences are shown in the thermal degradation behaviors of the different HBCD samples. At the end of the TG runs in pure nitrogen, HBCD samples yield a black solid residue (named char in the following), which corresponds to about 6% of the initial sample weight.

The results of isothermal TG runs performed on the HBCD samples in the range of 200 to 260 °C, reported in Figure 4, clearly show the presence of an autoaccelerating decomposition process. The autoaccelerating behavior of HBCD decomposition was also reported in other studies[16] and was attributed to the role of organic intermediate decomposition products.[13]

To better compare the current results with those present in the literature, a first-order autocatalytic kinetic model was fit to the isothermal TG data. The actual decomposition process was lumped into a simplified single-step reaction

$$\text{HBCD} \rightarrow \text{volatiles} + \text{char}$$

The following kinetic expression was derived for the HBCD conversion rate

$$\frac{d\xi}{dt} = K_d(T)\xi(1-\xi) = A_d e^{(-E_a/RT)}\xi(1-\xi) \qquad (5)$$

where K_d is an apparent kinetic constant; A_d is the frequency factor; E_a is the activation energy of the reaction; R is the gas constant; T is the temperature; and ξ, the sample conversion, is defined as

$$\xi = \frac{W_0 - W}{W_0 - W_f} \qquad (6)$$

where W is the sample weight, W_0 is the initial weight, and W_f is the final weight in the temperature range considered (200−260 °C).

Integration of eq 5 yields the following expression for the conversion as a function of time at constant temperature

$$\xi(t) = \frac{\xi_0 e^{K_d t}}{1 - \xi_0(1 - e^{K_d t})} \qquad (7)$$

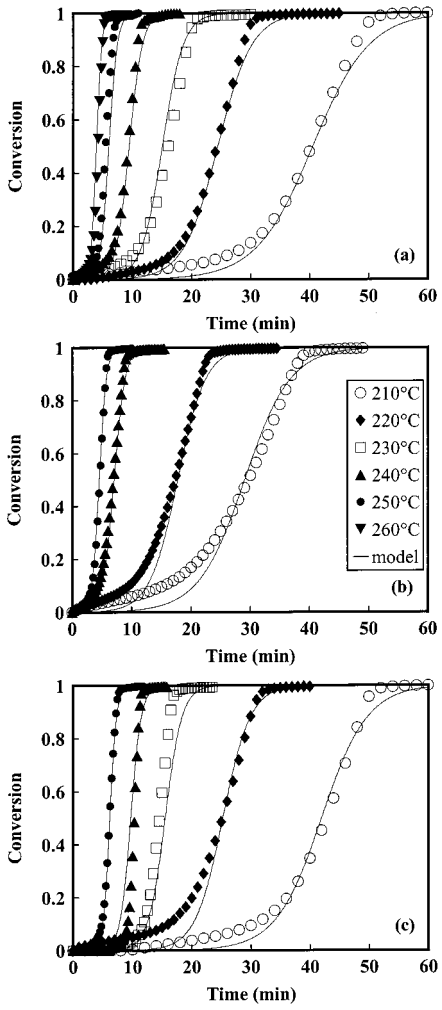

Figure 4. Results of isothermal TG runs for the HBCD samples: (a) HBCD1, (b) HBCD2, (c) HBCD3. Dots, experimental data; lines, kinetic model predictions.

where ξ_0 represents the initial weight fraction of catalytic species (originally present in the sample or formed before the beginning of HBCD decomposition). The value of the kinetic constant can be obtained from the experimental data using the following expression, derived from the integration of eq 5

$$K_d(T) = \frac{1}{t}\ln\left(\frac{\frac{\xi}{1-\xi}}{\frac{\xi_0}{1-\xi_0}}\right) \qquad (8)$$

where t is the experimental value of the time at which sample conversion ξ is accomplished. At constant temperature, the plot of K_d vs t calculated from the experimental data showed a negligible influence on the value of the kinetic constant. In contrast with the data of Larsen and Ecker,[13] no evidence of change in the apparent decomposition rate at high conversion values was found. Thus, the values of K_d calculated from experimental data at $\xi = 0.5$ were used for kinetic evaluations. The apparent kinetic parameters and ξ_0 where thus estimated by a best-fit procedure. Table 3 reports the values calculated for all of the HBCD samples. Figure 5 shows the Arrhenius plot (logarithm of the kinetic constant versus the reciprocal of temperature) obtained for the materials. The good accord

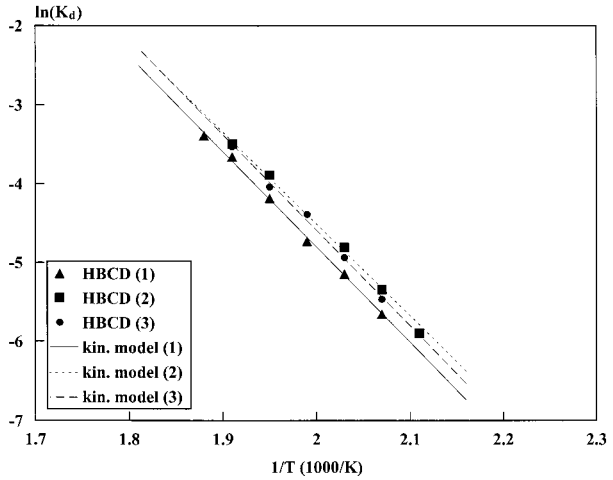

Figure 5. Arrhenius plot for HBCD decomposition.

shown in Figure 5 by the experimental data and the model results supports the adequacy of the simplified kinetic model used for the interpretation of the weight loss data. A further confirm comes from Figure 4, where the model predictions are compared with the experimental TG weight loss curves obtained for the three HBCD samples.

The values obtained for the activation energy in the present work are well within the range of those reported in the literature, which range between 92 and 130 kJ/mol depending on the data analysis procedure used.[13]

The analysis of the apparent kinetic parameters in Table 3 points out that the activation energies of the thermal decomposition process are quite similar for all of the HBCD samples. The lower thermal stability of HBCD2 resulted in higher values of the preexponential factor and the initial conversion parameter, ξ_0. Also in the work of Larsen and Ecker,[13] similar values of the activation energies were estimated for the decomposition of HBCD samples of quite different thermal stabilities.

Some authors suggest that the variations in the thermal stability of commercial HBCD samples might be caused by their different isomeric compositions, the γ isomer being the most thermally stable.[13,14] However, even if sample HBCD3 was composed only of the γ isomer, no relevant differences in the thermal stability with respect to that of sample HBCD1 were found, as shown in Figures 3 and 4. These results are in agreement with those of Peled et al.,[15] which suggest that a thermal rearrangement takes place, resulting in a constant distribution of the isomeric composition at the decomposition temperature.

Therefore, all of these data suggest that the thermal decomposition mechanism might be the same for the different HBCD materials. The lower thermal stability of HBCD2 seems to be attributable to a higher presence of impurities with a catalytic role in the decomposition process of this commercial product. This results in higher values of A_d and ξ_0 in the apparent kinetic model of the decomposition process. In fact, the influence of impurities on the thermal stability of HBCD is widely recognized in the literature.[13,16]

Thermal Effects of HBCD Decomposition. The DSC curve reported in Figure 3c for the three HBCD samples shows two well-defined endothermic peaks. The first endothermic peak is in the range of the melting point of HBCD. The second peak is caused by the decomposition process, as shown by the weight loss curves in Figure 3a. From baseline subtraction and integration of the heat flow curve, the estimation of the endothermic heat of decomposition of the HBCD samples was possible. The results are reported in Table 2.

Table 2. Apparent Kinetic Parameters and Overall Thermal Effects of HBCD Decomposition

	E_a (kJ/mol)	A (s^{-1})	ξ_0	ΔH (J/g)
HBCD1	103.3	1.37×10^8	2×10^{-4}	212.3
HBCD2	101.8	4.23×10^8	6×10^{-4}	208.9
HBCD3	102.3	3.16×10^8	4×10^{-5}	214.6

To determine whether the thermal effects of the decomposition process are dependent on temperature, semi-isothermal simultaneous TG/DSC runs were performed at temperatures between 200 and 225 °C. No relevant differences were detected in the estimated values of the decomposition heat with respect to the DSC constant-heating-rate runs, thus confirming that the HBCD decomposition process is endothermic and that the reaction heat is not significantly influenced by the decomposition temperature in the 200−250 °C range.

No data are reported in the literature on the thermal effects of HBCD decomposition. However, some authors have suggested that the first step involved in HBCD thermal degradation is the formation of radicals.[13,14] This might explain the above results, as radical formation is an endothermic process.

In the case of HBCD, the time to maximum rate is not a significant parameter for the characterization of the thermal stability of the substance, as the decomposition in an open system is endothermic. However, on the basis of the above results, the thermal stability of HBCD can be defined using the onset temperature calculated from constant-heating-rate DSC data. A value of 253 °C was obtained for HBCD1 at a heating rate of 10 °C/min.

Safe process temperatures are strictly dependent on process characteristics and conditions. Nevertheless, the determination of a reference threshold value, above which relevant decomposition phenomena should be expected, might be useful as a preliminary indication of safe operating temperatures for industrial processes involving HBCD. A reference temperature threshold value was defined as the temperature at which a 1% weight loss takes place in 5 min. This can be calculated from eq 8, assuming $\xi = 0.01$ and $t = 300$ s, resulting in a value of 235 °C for HBCD1.

Decomposition Products of HBCD. TG-FTIR and FBR runs allowed for the characterization of the HBCD thermal degradation products at the low heating rates (10 °C/min) used in the present study. All of the data reported in this section are the results of experimental runs performed on HBCD1. However, negligible differences were found using the HBCD2 and HBCD3 samples.

Figure 6 shows the results of FTIR on-line analysis of the volatiles evolved in TG-FTIR runs. The IR spectra recorded at regular intervals of 9.5 s are reported as a function of the temperature of the sample in the TG furnace. Hydrogen bromide and hydrocarbon compounds were the only decomposition products identified in the TG-FTIR runs. Using the data in Figure 6, qualitative emission profiles as a function of temperature were obtained for these compounds following the procedure discussed in the Experimental Section. Figure 7a shows the evolution profiles for hydrogen bromide and hydrocarbon compounds identified by the absorption over the

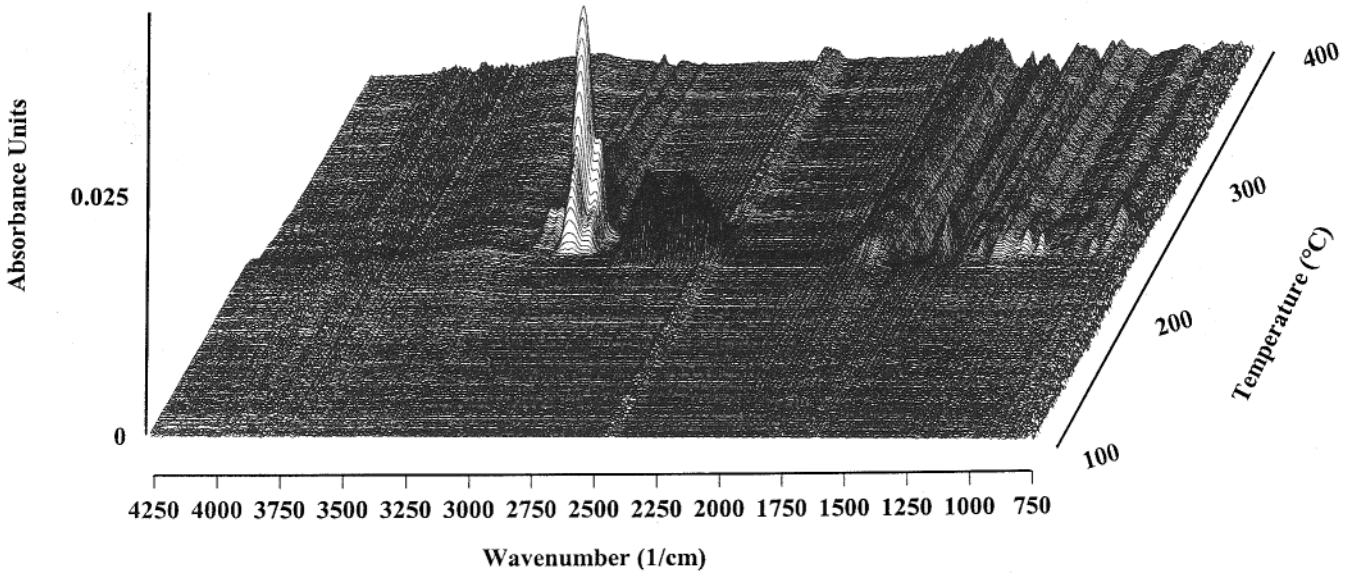

Figure 6. IR spectra collected in a TG-FTIR run carried out on a HBCD1 sample (10 °C/min, 40−500 °C, 100% nitrogen).

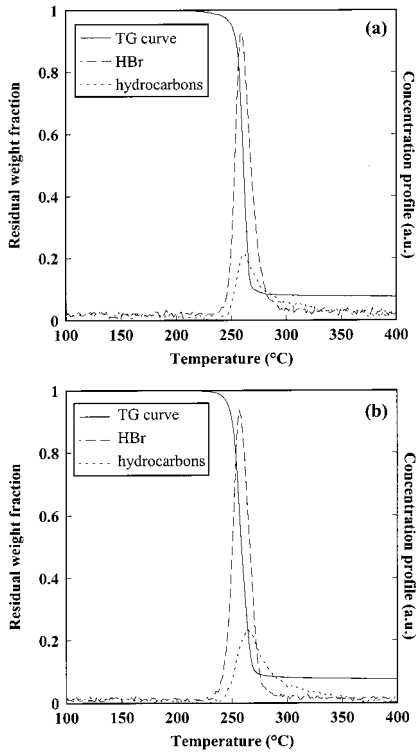

Figure 7. Profiles of hydrogen bromide and hydrocarbon compound formation during HBCD decomposition in TG-FTIR runs (10 °C/min, 40−500 °C): (a) 100% nitrogen, (b) air.

selected wavenumber intervals, as reported in the Experimental Section. The figure confirms that HBCD decomposition takes place in a single stage and that no significant differences can be observed between the temperature ranges of formation of hydrogen bromide and hydrocarbon compounds.

The results of the FBR runs carried out in 100% nitrogen at a heating rate of 10 °C/min confirmed the presence of hydrogen bromide among the gaseous decomposition products. FTIR off-line analyses were carried out using the D1 cell (see Figure 1) at 5-min intervals. However, no hydrocarbon compounds were detected in these measurements.

It must be remembered that, in TG/FTIR runs, the TG furnace is connected to the FTIR analyzer by a transfer line heated at 200 °C, whereas in FBR runs the gas flows through a surface condenser at a temperature of −20 °C (E1) before entering the D1 gas sampling cell. Thus, the absence of C−H stretching absorptions in the FTIR spectra during the FBR runs might well suggest that only hydrocarbon compounds with low volatility are formed in HBCD decomposition and that they are condensed in the E1 trap without entering the D1 gas cell.

As stated in the Experimental Section, the identification of hydrocarbon compounds by FTIR analysis was not possible. This identification was afforded, instead, by GC/MS analysis of the E1 condensate, performed following the procedure described in the Experimental Section.

A total of 174 compounds were separated by the GC column. Most of them were identified by comparison with NIST library MS spectra and by the use of standards; the others were identified by analysis of the mass spectra and fragmentation patterns.

Table 3 reports the compounds identified as having three or more bromine atoms. Table 4 summarizes the more important categories of identified compounds having two or fewer bromine atoms.

Tables 3 and 4 clearly show that most of the identified compounds have 12 carbon atoms, suggesting that intramolecular reactions are the main pathway of HBCD thermal degradation. The quite limited number of compounds in Table 3 suggests that hydrogen bromide loss resulting in unsaturation is the main decomposition reaction up to the formation of three unsaturated bonds in the C_{12} ring.

The presence of TBCD, tribromocyclododecadiene, and tribromocyclododecene might be caused by Br_2 elimination.[23] However, TBCD is an impurity of HBCD; thus, its presence in the condensate might not be due to the thermal degradation of HBCD. This hypothesis is supported by the fact that no evidence for relevant formation of Br_2 was obtained by the analysis of the C1 and C2 scrubber solutions at the end of pyrolysis runs by the procedures described in the Experimental Section. The presence of TBCD, and thus of its decomposition products, might also explain the presence of tribromo-

Table 3. Thermal Degradation Products of HBCD with Three or More Bromine Atoms Formed in 100% Nitrogen FBR Runs and Identified by GC/MS Analysis

number of Br atoms	number of C atoms	compound (number of isomers)	MW (g/mol)
tribrominated	C_{12} compounds	tribromohexahydrobenzocyclooctene (3)	397
		tribromocyclododecatriene (4)	399
		tribromocyclododecadiene (16)	401
		tribromocyclododecene (2)	403
tetrabrominated	C_{12} compounds	tetrabromocyclododecadiene (13)	480
		tetrabromocyclododecene (10)	482
pentabrominated	C_{12} compounds	pentabromocyclododecene (7)	561

Table 4. Thermal Degradation Products of HBCD with Less than Three Bromine Atoms Formed in 100% Nitrogen FBR Runs and Identified by GC/MS Analysis

number of Br atoms	number of C atoms	compound class (number of compounds/isomers)
nonbrominated	C_8 compounds	alkyl-substituted benzene (4)
	C_9 compounds	alkyl-substituted benzene (2)
	C_{10} compounds	naphthalene (1)
	C_{11} compounds	methylnaphthalene (2)
	C_{12} compounds	cyclododecatriene (2)
		5,6,7,8,9,10-hexahydrobenzocyclooctene (1)
		alkyl-substituted benzene (7)
		biphenyl (1)
		biphenylene (1)
		alkyl-substituted naphthalene (10)
		1,2,3,4-tetrahydro-1,4-ethanonaphthalene (1)
		acenaphthene (1)
		acenaphthylene (1)
		1,2,2A,3,4,5-hexahydroacenaphthylene (1)
		1,2,3,6,7,8-hexahydro-as-indacene (1)
		tricyclo-7.3.0.0.(2,6)−7-dodecene (1)
		4.4.2-propella-3,8,11-triene (1)
monobrominated	C_{10} compounds	bromonaphthalene (2)
	C_{12} compounds	bromocyclododecadiene (1)
		bromocyclododecatriene (6)
		bromohexahydrobenzocyclooctene (2)
		bromocyclohexadienylbenzene (1)
		bromobiphenyl (2)
		bromodimethylnaphthalene (2)
		bromoethyltetrahydronaphthalene (1)
		bromoacenaphthene (1)
		bromoacenaphthylene (1)
		bromohexahydro-as-indacene (3)
dibrominated	C_{12} compounds	dibromocyclododecadiene (7)
		dibromocyclododecatriene (7)
		dibromohexahydrobenzocyclooctene (3)
		dibromobiphenyl (1)

cyclododecadiene among the compounds identified in Table 3. In fact, tribromocyclododecadiene can easily be formed from TBCD by a dehydrobromination reaction. If this is the case, then the reactive pathway originally proposed by Larsen and Ecker[13] for HBCD decomposition (Scheme 1) has found experimental support, as all of its intermediates were identified in the present work. Furthermore, intramolecular reaction processes might well explain the formation of most of the categories of compounds formed in HBCD decomposition: brominated haxahydrobenzocyclooctenes (Scheme 1), hexahydro-as-indacenes (Scheme 2), biphenyls (Scheme 3), and dimethylnaphthalenes (Scheme 4). The products identified by GC/MS analysis are indicated by an asterisk in the schemes.

Schemes 1−4, all leading to identified products, represent the main reaction pathways involved in HBCD primary pyrolysis well. HBCD appears to decompose by a complex mechanism involving dehydrobromination reactions,[24] Diels−Alder reactions, and radical reactions.[25,26] An important feature of the process is that the intramolecular reactions prevail over intermolecular pathways, at least for the conditions studied herein. Thus, the loss of three atoms of bromine,

Scheme 1

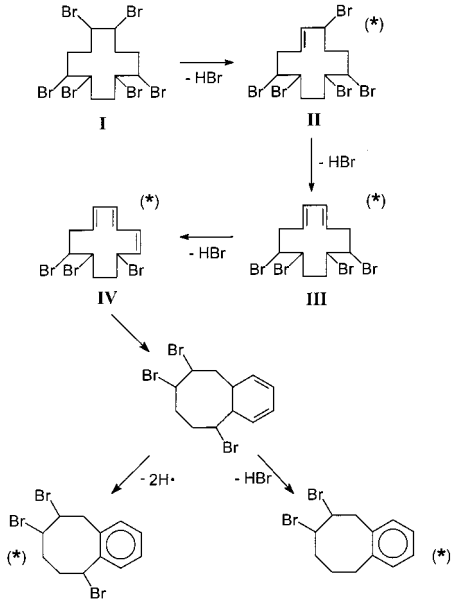

Scheme 2

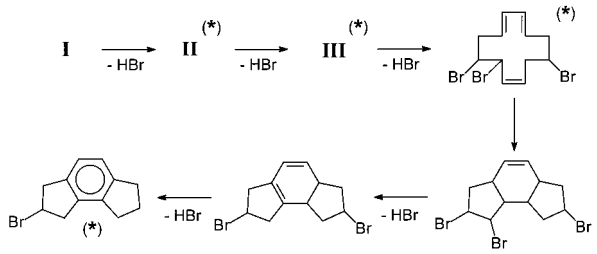

Scheme 3

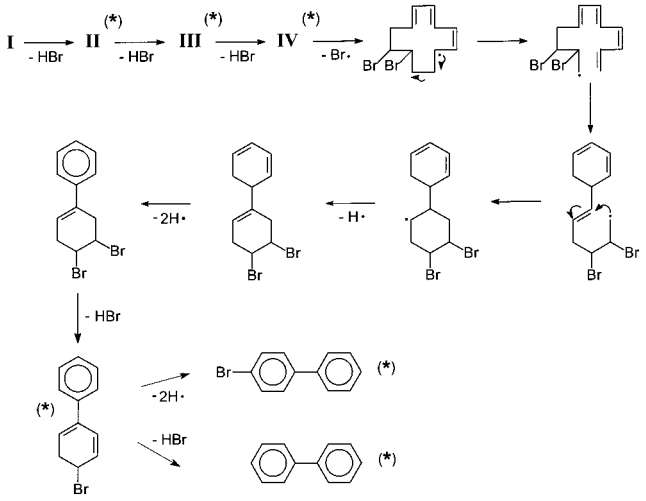

Scheme 4

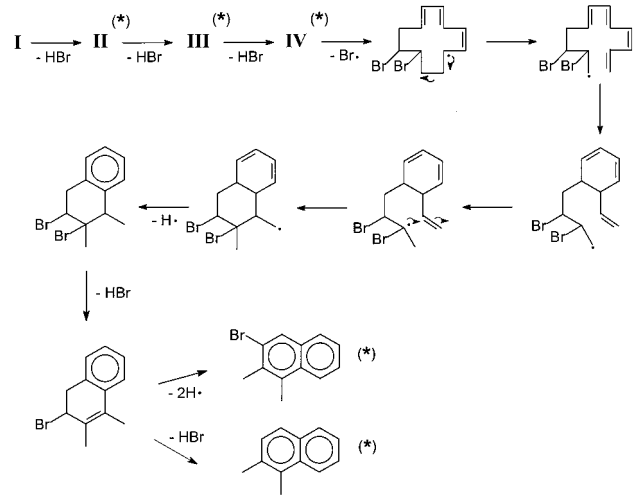

yielding tribromocyclododecatriene, seems to be the main pathway leading to the formation of decomposition products. This strongly suggests that aromatic structures such as biphenyls or naphthalenes formed during HBCD decomposition are mainly mono-, bi-, or tribrominated. The direct formation of tetrabrominated aromatic structures seems not to be favored in HBCD thermal degradation. The decomposition mechanism hypothesized seems to suggest that the formation of such compounds, if present, might take place mainly by a secondary reaction process due to the bromination of aromatic rings by bromine radicals that might be formed in the decomposition.

Distribution of Bromine among Thermal Decomposition Product Fractions. Quantitative data on the bromine distribution among the different fractions of decomposition products formed are strictly related to the experimental conditions used in the present study. However, even in light of this limitation, it is interesting to estimate the quantities of HBr formed in HBCD decomposition, as this compound seems to be the main cause of the flame-retardant properties of HBCD. On the other hand, bromine not released as hydrogen bromide might contribute to the formation of high-molecular-weight aromatic and polyaromatic brominated decomposition products, such as those identified in Table 4.

Table 5. Bromine Distribution in the Product Fractions Obtained from HBCD Thermal Degradation

		fraction of sample initial mass (wt %)	fraction of bromine initially present (wt %)	bromine content (wt %)
HBCD		100	100	74.6
decomposition in 100% N_2	HBr	58	77	98.8
	condensables	36	23	48
	char	6	0	0
decomposition in air	HBr	57	76	98.8
	condensables	37	24	48
	char	6	0	0

TG-FTIR results were used to obtain data on the quantities of hydrogen bromide formed in HBCD decomposition. Calibration data allowed for the estimation of the quantities of HBr formed during TG-FTIR runs at 10 °C/min by the procedure discussed in the Experimental Section. As shown in Table 5, the amount of HBr formed is about 58% of the HBCD initial weight, which corresponds to 77% of the bromine initially present in the sample. This value was obtained as the mean of five experimental runs, with errors of less than 3 wt %.

These data were confirmed by the results of the FBR runs. At the end of the FBR experiments, the solutions present in absorbers C1 and C2 were titrated for NaOH excess using a hydrochloric acid solution, to estimate the total amount of HBr formed. The results indicated the formation of 57.6% HBr with respect to the initial HBCD weight (value obtained as a mean of five experimental runs, with errors of less than 3 wt %). This result is in good agreement with the data obtained from the TG-FTIR runs, thus confirming the validity of the approach developed for the quantitative analysis of TG-FTIR data. Furthermore, these data are sufficiently close to those obtained by Larsen and Ecker,[13] which detected the formation of 62.5 wt % HBr in the pyrolysis of HBCD samples under isothermal conditions at 195 °C.

As previously mentioned, no other gaseous products were identified during HBCD degradation. The formation of significant quantities of Br_2 (which can not be identified by IR techniques) was excluded by iodometric titration (see the Experimental Section). Thus, it can be inferred that the bromine that is not released as hydrogen bromide should be mainly contained in the condensable volatile products and in the solid residue present on the sample holder of the FBR at the end of the run. The weight of the solid residue amounted to about 6% of the intial HBCD sample weight in both the FBR and the TG-FTIR runs.

The bromine content of the pyrolysis residue was determined by combustion followed by argentimetric titration (Volhard method[19]). The results are reported in Table 5. As shown in the table, a mass balance on the recovered product fractions allows for the estimation

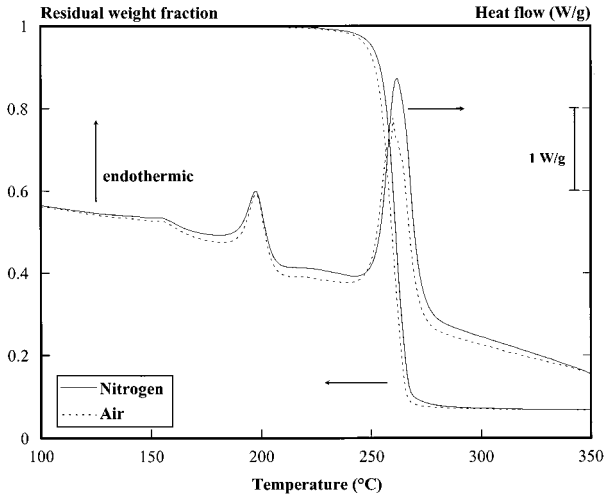

Figure 8. Results of simultaneous TG/DSC runs carried out on HBCD1 samples at a heating rate of 10 °C/min.

of the distribution of bromine among the different product fractions. The data obtained show that volatiles formed at the low heating rates used here, which represent 36 wt % of the HBCD, contain approximately 23% of the bromine initially present in HBCD.

Influence of Oxygen on the Thermal Decomposition. To investigate the influence of oxidizing conditions on HBCD thermal stability, constant-heating-rate TG/DSC runs were performed. An endothermic heat of 195.7 J/g was determined, very similar to the values reported in Table 2. TG-FTIR and FBR experimental runs were performed on HBCD1 using air (21 mol % oxygen) as the purge gas.

The TG and DSC data obtained for HBCD1 are reported in Figure 8. A comparison of the TG and DSC curves in air with those obtained in 100% nitrogen, also reported in the figure, clearly shows that no relevant differences appear in the weight loss and decomposition thermal effects at a heating rate of 10 °C/min. Similar results were obtained for the other HBCD samples.

The TG-FTIR data confirmed that no relevant differences occur in the primary thermal decomposition process when oxygen is present. Figure 7b reports the evolution profiles of HBr and hydrocarbons. Negligible differences appear with respect to the data reported in Figure 7a for the TG-FTIR runs in pure nitrogen.

Quantitative FTIR data were used to estimate the quantity of hydrogen bromide formed during HBCD decomposition. The results obtained, reported in Table 5, clearly show that no relevant differences could be observed in the formation of hydrogen bromide in the presence of air.

FBR runs were performed using 6 and 21 vol % oxygen/nitrogen mixtures. The condensable fraction recovered was analyzed by GC/MS. No relevant differences were found in the identified compounds with respect to those reported in Tables 3 and 4.

Thus, these results suggest that, at the low heating rates used in the experimental runs (10 °C/min), the primary decomposition process of HBCD is not significantly influenced by the presence of air. The presence of air is assumed to influence mainly the secondary gas-phase reactions, which in the FBR are quenched by the low temperatures and the low residence time of the gas phase inside the hot zone of the reactor. This is a typical result for the primary thermal degradation process of organic substances and polymers where a large amount of volatile products are formed. Oxygen diffusive limitations due to the flow of primary decomposition products formed during HBCD degradation possibly contribute to the phenomenon, reducing the oxygen concentration at the sample surface.

However, these results also suggest that the data obtained on the primary degradation process might have a general validity in explaining the primary decomposition pathways of HBCD thermal decomposition. Furthermore, the data reported above seem to suggest that the formation of polybrominated substances (such as PBDF and PBDD) during HBCD decomposition in an oxidizing atmosphere, when it occurs, might take place mainly as a result of secondary gas-phase reaction processes. Thus, the formation of mono-, di-, and tribrominated polyaromatic structures seems to be favored, as discussed above. These findings are in agreement with the results of previous studies,[5] which identified only mono-, di-, and tribrominated dibenzodioxins in the combustion products of HBCD in polymer matrixes.

Conclusions

HBCD thermal stability and decomposition pathways were investigated by combined experimental techniques. HBCD thermal degradation showed an autoaccelerating behavior, possibly catalyzed by organic intermediates formed in the decomposition process. The thermal stability was found to be influenced by sample purity. On the other hand, the results obtained suggested a limited effect of isomeric composition of the HBCD sample on the decomposition temperatures.

An analysis of the HBCD thermal decomposition products was carried out by the TG-FTIR and GC/MS techniques. The use of standard samples and the analysis of mass fragmentation spectra allowed for the identification of polybrominated organic substances formed in the primary pyrolysis process at moderate heating rates (10 °C/min). The presence of oxygen was found to have a negligible influence on the degradation products obtained during HBCD decomposition, at least at the heating rates used in this study.

Quantitative data on hydrogen bromide formation and on the bromine distribution among the different product fractions were obtained either by TG-FTIR or by FBR runs. The data confirmed that about 75% of bromine by weight is released as HBr and showed that 25% is involved in the formation of high-molecular-weight bromo-organic compounds (35% of the initial HCBD weight).

On the basis of the identified products, the main pathways of HBCD thermal degradation could be investigated and a global mechanism for HBCD decomposition was proposed.

The results obtained indicate that hexa-, penta-, and tetrabrominated polyaromatic structures are not primary products of HBCD decomposition and might be obtained mainly by secondary bromination reactions.

Acknowledgment

The authors gratefully acknowledge financial support from CNR−Gruppo Nazionale di Ricerca per la Difesa dai Rischi Chimico-Industriali ed Ecologici.

Nomenclature

A = absorbance
A_d = preexponential factor, s^{-1}

C = concentration, mol/L
D = integral of I with respect to time, $cm^{-1}s$
E_a = activation energy, kJ/mol
I = integrated absorbance, cm^{-1}
K = experimental constant relating I to concentration, $cm^{-1}mol^{-1}$ L
K_d = kinetic constant, s^{-1}
l = optical path length, cm
MW = molecular weight, g/mol
P = total amount of compound evolved, mol
Q = volumetric gas flow rate, L/s
R = universal gas constant, 8.31 J/(mol K)
t = time, s
T = temperature, K
W = sample weight, g
ΔH = heat of decomposition, J/g
ϵ = extinction coefficient, $cm^{-1}mol^{-1}$ L
ν = wavenumber, cm^{-1}
ξ = conversion

Literature Cited

(1) Pettigrew, A. Halogenated Flame Retardants. In *Encyclopedia of Chemical Technology*, 4th ed.; Kirk, R. E., Othmer, D. F., Eds.; John Wiley & Sons: New York, 1993; Vol. 10, p 954.

(2) Buser, H. R. Polybrominated Dibenzofurans and Dibenzo-*p*-dioxins: Thermal Reaction Products of Polybrominated Diphenyl Ether Flame Retardants. *Environ. Sci. Technol.* **1986**, *20*, 404.

(3) Thoma, H.; Hutzinger, O. Pyrolysis and GC/MS analysis of brominated flame retardants in on-line operation. *Chemosphere* **1987**, *16*, 1353.

(4) Bienek, D.; Bahadir, M.; Korte, F. Formation of heterocyclic hazardous compounds by thermal degradation of organic compounds. *Heterocycles* **1989**, *28*, 719.

(5) Dumler, R.; Thoma, H.; Lenoir, D.; Hutzinger, O. PBDF and PBDD from the combustion of bromine containing flame retarded polymers: A survey. *Chemosphere* **1989**, *19*, 2023.

(6) McAllister, D. L.; Mazac, C. J.; Gorsich, R.; Freiberg, M.; Tondeur, Y. Analysis of polymers containing brominated diphenyl ethers as flame retardants after molding under various conditions. *Chemosphere* **1990**, *20*, 1537.

(7) Dumler, R.; Lenoir, D.; Thoma, H.; Hutzinger, O. Thermal formation of polybrominated dibenzofurans and dioxins from decabromodiphenyl ether flame retardant: Influence of antimony(III) oxide and the polymer matrix. *Chemosphere* **1990**, *20*, 1867.

(8) Thies, J.; Neupert, M.; Pump, W. Tetrabromobisphenol A (TBBA), its Derivatives and their Flame Retarded (FR) Polymers: Content of Polybrominated Dibenzo-*p*-Dioxins (PBDD) and Dibenzofurans (PBDF). *Chemosphere* **1990**, *20*, 1921.

(9) Luijk, R.; Wever, H.; Olie, K.; Govers, H. A. J.; Boon, J. J. The influence of the polymer matrix on the formation of polybrominated dibenzo-*p*-dioxins (PBDDs) and polybrominated dibenzofurans (PBDFs). *Chemosphere* **1991**, *23*, 1173.

(10) Striebich, R. C.; Rubey, W. A.; Tirey, D. A.; Dellinger, B. High-temperature degradation of polybrominated flame retardant materials. *Chemosphere* **1991**, *23*, 1197.

(11) Luijk, R.; Govers, H. A. J. The formation of polybrominated dibenzo-*p*-dioxins (PBDDs) and dibenzofurans (PBDFs) during pyrolysis of polymer blends containing brominated flame retardants. *Chemosphere* **1992**, *25*, 361.

(12) Riess, M.; Ernst, T.; Popp, R.; Schubert, T.; Thoma, H.; Vierle, O.; Ehrenstein, G. W.; Van Eldik, R. Analysis of flame retarded polymers and recycling materials. *Organohalogen Compd.* **1998**, *35*, 443.

(13) Larsen, E. R.; Ecker, E. L. Thermal Stability of Fire Retardants: I. Hexabromocyclododecane (HBCD). *J. Fire Sci.* **1986**, *4*, 261.

(14) Larsen, E. R.; Ecker, E. L. Thermal Stability of Fire Retardants: III. Decomposition of Pentabromochlorocyclohexane and Hexabromocyclododecane under Processing Conditions. *J. Fire Sci.* **1988**, *6*, 139.

(15) Peled, M.; Scharia, R.; Sondack, D. Thermal Rearrangement of Hexabromocyclododecane (HBCD). In *Advances in Organobromine Chemistry II*; Elsevier Publishers: New York, 1995; p 92.

(16) Reyes, J. D.; Scheinert, J.; Georlette, P. HBCD: Advancing Performance through Innovation. *Recent Adv. Flame Retard. Polym. Mater.* **1997**, *8*, 390.

(17) Cozzani, V.; Petarca, L.; Tognotti, L. Devolatilization and Pyrolysis of Refuse Derived Fuel: Characterization and Kinetic Modelling by a Thermogravimetric and Calorimetric Approach. *Fuel* **1995**, *74*, 903.

(18) Feigl, F. *Spot Tests*, 4th ed.; Elsevier Publishing Company: Amsterdam, The Netherlands, 1954; Vol. 1, p 337.

(19) Skoog, D. A.; West, D. M.; Holler, F. J. *Fundamentals of Analytical Chemistry*, 6th ed.; Saunders College Publishing: Philadelphia, PA, 1992.

(20) Potts, W. J., Jr. *Chemical Infrared Spectroscopy*; John Wiley & Sons: New York, 1963.

(21) Bak, J.; Larsen, A. Quantitative Gas Analysis with FT-IR: A Method for CO Calibration Using Partial Least-Squares with Linearized Data. *Appl. Spectrosc.* **1995**, *49*, 437.

(22) Pecori, L. Aspetti di sicurezza legati alla formazione ed al rilascio di composti bromurati in incidenti. M.S. Thesis in Chemical Engineering, University of Pisa, Pisa, Italy, 2000.

(23) Baciocchi, E. 1,2-Dehalogenations and related reactions. In *The Chemistry of Halides, Pseudo-Halides and Azides*; Patai, S., Rappoport, Z., Eds.; John Wiley & Sons: New York, 1983; p 161.

(24) Egger, K. W.; Cocks, A. T. Pyrolysis reactions involving carbon−halogen bonds. In *The Chemistry of Carbon−Halogen Bonds*; Patai, S., Ed.; John Wiley & Sons: New York, 1973; p 677.

(25) Rebick, C. Pyrolysis of Heavy Hydrocarbons. In *Pyrolysis: Theory and Industrial Practice*; Albright, L. F., Crynes, B. L., Corcoran, W. H., Eds.; Academic Press: New York, 1983; p 69.

(26) Sakai, T. Thermal Reaction of Olefins and Diolefins, and Formation of Aromatics. In *Pyrolysis: Theory and Industrial Practice*; Albright, L. F., Crynes, B. L., Corcoran, W. H., Eds.; Academic Press: New York, 1983; p 89.

Received for review November 27, 2000
Revised manuscript received March 30, 2001
Accepted May 8, 2001

IE001002V